IMPACTS OF TOPOGRAPHIC SHADING ON SURFACE ENERGY BALANCE OF HIGH MOUNTAIN ASIA GLACIERS

by

Matthew Howard Olson

A thesis submitted to the faculty of
The University of Utah
in partial fulfillment of the requirements for the degree of

Master of Science

Department of Geography

The University of Utah

August 2017

The University of Utah Graduate School

STATEMENT OF THESIS APPROVAL

The thesis of Matthew Howard Olson

has been approved by the following supervisory committee members:

Summer Rupper	, Chair	**04/27/17** Date Approved
Richard Forster	, Member	**04/27/17** Date Approved
Simon Brewer	, Member	**04/27/17** Date Approved

and by **Andrea Brunelle**, Chair/Dean of

the Department/College/School of **Geography**

and by David B. Kieda, Dean of The Graduate School.

ABSTRACT

Topographic shading involves two components: shaded relief and cast shadowing. Shaded relief occurs from self-shadowing due to the slope and aspect of a given location; cast shadowing involves projecting shade from nearby terrain onto an adjacent surface. The combined effect of topographic shading plays a fundamental role in determining surface energy balance for glacier ice. However, this parameter has been oversimplified or incorrectly incorporated in some past studies. Here we develop a topographic solar radiation model to examine the variability in mean irradiance throughout the melt season due to topographic shading and combined slope and aspect. We utilize the 30-meter resolution ASTER GDEM and multihour solar geometry to simulate topographic shading on two glaciers of differing morphologies in regions of contrasting terrain. We test the sensitivity of shading to valley-aspect and latitude for the same two glaciers, and observe patterns in these parameters for a suite of glaciers across High Mountain Asia (HMA). Our results show that topographic shading significantly alters the potential direct clear-sky solar radiation received at the surface for valley glaciers in HMA. Additionally, contrary to the findings of some previous studies, we find that shading can be extremely impactful in the ablation zone of some valley glaciers, particularly for north- and south-facing valleys. A daily mean change in irradiance of more than -70 Wm^{-2} due to cast shadowing is found in the ablation zones of some HMA glaciers. Cast shadowing is the dominant mechanism in determining total shading for valley glaciers in parts of HMA,

especially at lower elevations. Although shading has some predictable characteristics, it is overall extremely variable between glacial valleys, and therefore very difficult to parameterize. We use a modified temperature-index model that includes potential clear-sky irradiance to calculate melt for one selected glacier. Excluding topographic shading for this glacier results in an overestimation of total summer melt in the ablation zone by up to 10%. This demonstrates that topographic shading is not only an important factor contributing to surface energy balance, but can also influence the mass balance of glaciers throughout HMA.

TABLE OF CONTENTS

LIST OF FIGURES

Figures

ACKNOWLEDGMENTS

We acknowledge the support for this research through funding awarded to Summer Burton Rupper (NSF EAR 1600587 and NASA 15-HMA15-0030). This work benefitted greatly from tools developed by Javier Corripio (2003), as well as data from the International Centre for Integrated Mountain Development, the Randolph Glacier Inventory, and the Advanced Spaceborne Thermal Emission and Reflectance Radiometer (30m).

CHAPTER 1

INTRODUCTION

Valley glaciers are an important source of freshwater for many local communities. Summer melt water is vital for irrigation and drinking sources in some regions (Immerzeel et al., 2010). Additionally, after thermal expansion, mountain glaciers are expected to be the next biggest contributor to sea-level rise over the next century (IPCC, 2014). Improvement to our understanding of these glacial systems is essential in properly quantifying melt and associated impacts, particularly in remote regions where in situ data is sparse.

1.1 Energy Balance and Global Radiation

The surface energy balance of a glacier controls melt, and is therefore directly related to the glacier mass balance. Energy balance is the sum of energy inputs to the surface of a glacier, which can be represented simplistically as:

$$Q_m = S_{net} + L_{net} + Q_H + Q_L \quad (1)$$

where Q_m is the energy available to melt, S_{net} is net shortwave radiation, L_{net} is net longwave radiation, Q_H is sensible heat, and Q_L is latent heat. While other energy fluxes exist on glacier surfaces, these four components dominate the glacier energy budget for most glaciers. When Q_m is positive, excess energy entering the system leads to an increase in surface temperature when the ice temperature is below the melting point, and melt on the surface when the ice temperature is equal to zero. When Q_m is negative, the glacier surface decreases in temperature. The turbulent fluxes (Q_H and Q_L) are largely a function of near surface temperature and humidity gradients. Changes in net radiation at the surface, such as a decrease in shortwave radiation due to topographic shading, can alter these near surface gradients (Arnold et al., 2006).

During the summer months, net shortwave radiation on a glacier is one of the main components of surface energy balance, often accounting for 75% or more of available energy at the surface (Arendt et al., 1999; Gruell & Smeets, 2001; Oerlemans & Klok, 2002). The shortwave component of energy balance relies on surface albedo and the amount of incoming global radiation, Q_{Global}, which is defined as:

$$Q_{Global} = I + D_s + D_t \tag{2}$$

where I is direct solar radiation, D_s is diffuse sky radiation, and D_t is terrain reflected radiation. Diffuse sky radiation provides a small, but potentially significant, contribution to global radiation. Terrain reflected radiation can also be significant in regions surrounded by highly reflective terrain or areas of dense vegetation (Dozier et al., 1980). However, the bulk of the energy flux into the system during the melt season is largely determined by changes in direct solar radiation (Arnold et al., 2006). Therefore, any change to this component of energy will largely alter the overall global radiation, and consequently be a significant influence on surface energy balance.

1.2 Topographic Shading

Solar radiation is primarily a function of latitude and time of year, with parameters such as topographic shading, slope, and aspect controlling the distribution of radiation on a local scale. To first order, it is often assumed that shading from surrounding topography primarily alters daily solar radiation at higher elevations on a glacier surface, leaving the lower elevations mostly unaffected (Arnold et al., 2006). This leaves variation in daily solar radiation along a given elevation to be largely controlled by the slope and aspect on a glacier's surface. Klok et al. (2002) show that ignoring topographic effects such as shading, slope, aspect, and obstruction of the sky can result in a 37% overestimation of incoming solar radiation. This can introduce a large amount of error in calculating net shortwave radiation on a glacier surface. This is especially problematic in regions of extremely high, steep topography where direct solar radiation can be obstructed for almost the entire year (Aguilar et al., 2010). These studies strongly suggest that slope, aspect, and topographic shading can be an important piece of glacier energy balance.

We separate topographic shading into two components: shaded relief and cast shadow. Shaded relief occurs due to self-shadowing at a given location and relies solely on slope and aspect. In essence, shaded relief is a modification of the incident angle, which is the angle between surface normal (zenith) and the position of the sun at a given moment. If the angle of incidence for a particular cell is greater than 90°, it is labeled as "shadow," if less, it is considered "in sun" (Figures 1, 2). This method is also often used as an image enhancing technique for display purposes.

Cast shadows are a result of shading due to adjacent topography. Although a given slope may be facing the direction of incoming solar radiation, an adjacent topographic feature or valley wall may block the hillside from direct solar radiation (Figures 1, 2). Cast shadows are extremely important in regions of steep terrain and narrow valleys. Because local terrain is unique and solar angles vary constantly, cast shadows must be considered for each sun position over an hourly, daily, and monthly time interval (Aguilar et al., 2010). Dozier et al. (1981) provide an estimation of cast shadowing based on a horizon angle, defined as the angle between surface normal and the line joining a certain point with the highest visible point of topography in the direction of solar azimuth. This method has been used in some studies focused on glacier mass balance (Aguilar et al., 2010; Hock, 1997). An additional method for calculating cast shadows, is utilizing a modified ray-tracing algorithm to conclude whether a specific cell is obstructed from the solar position (Corripio, 2003; Gill, 2010).

With the global availability of 30-meter resolution digital elevation models (DEMs), slope and aspect can be easily incorporated in solar radiation calculations; however, topographic shading is often ignored or over-simplified in glacier energy balance calculations due in part to computational expense and complexity. While true topographic shading is often excluded, there are important exceptions as discussed above (e.g., Aguilar et al., 2010; Arnold et al., 2006; Dozier et al., 1981; Hock, 1997; Klok et al., 2002; Williams et al., 1972). However, many radiation models commonly used in glacier studies only incorporate shaded relief without including cast shadowing (Chen et al., 2013; Han et al., 2016; Hopkins et al., 2010; Kumar et al., 1997; Plummar et al., 2003; Zhang et al., 2015; and others). Even the ESRI Solar Radiation Toolbox only incorporates shaded relief, as it relies on the ESRI Hillshade algorithm to calculate topographic shading. Some of these models, which only include shaded relief, interpret topographic shading as an insignificant contribution to the overall radiation budget. This may be due to selecting study sites in areas of lower relief, or the fact that these models do not completely account for topographic shading.

It has often been assumed that topographic shading is only significant at steep, high elevations in the accumulation zone of a glacier, and that slope and aspect are the dominant topographic parameter in affecting solar radiation in mountainous terrain (Arnold et al., 2006; Dozier et al.,1981; Klok et al., 2002; Munro et al., 1982). Although this may hold true in certain regions of the world, other regions may be affected differently by topographic shading from steep terrain surrounding valley glacier peripheries. This study focuses on improving the current understanding of how topographic factors such as shaded relief, cast shadows, and slope and aspect influence glacier melt, specifically, how these topographic factors influence the distribution of direct solar radiation on glacier surfaces. We focus this study on glaciers in the complex and varied topography of High Mountain Asia (HMA).

1.3 High Mountain Asia

High Mountain Asia (HMA) is chosen as the regional focus of this study for several reasons. First, this region houses the largest volume of ice on the planet outside the polar regions (Bolch et al., 2012). Glacier melt throughout HMA is a vital water source for many downstream communities (Immerzeel et al., 2010), and changes in these glaciers contribute to eustatic sea-level rise (Gardner et al., 2013; Jacob et al., 2012). Despite the societal importance of these glaciers, mass balance estimates across the region are extremely sparse and vary from + 0.11 ± 0.22 to -0.85 m.w.e.a^{-1} (Bolch et al., 2012; Kaab et al., 2015). Thus, there is a need for large-scale glacier mass balance models in this region, including an improved understanding of the role of topographic shading. Second, glaciers in HMA span a wide spectrum of climatologies and topographies within the Asian continent. Thus, this region is ideal for assessing how the role of topographic shading varies across different topographic and climatic zones. Finally, HMA is known for dramatic mountain peaks, steep valley walls, and deep glaciated valleys. Thus, this is a region with high potential for topographic shading, both from shaded relief and cast shadows, which may have a significant impact on incoming solar radiation for HMA glaciers. The benefits of selecting glaciers in this region include improvements to modeling techniques for these remote but important glaciers, an improved understanding of how shading varies across different climatic and topographic settings, and a focused analysis in a region that has high potential for topographic shading but where little work has been done to assess the overall importance.

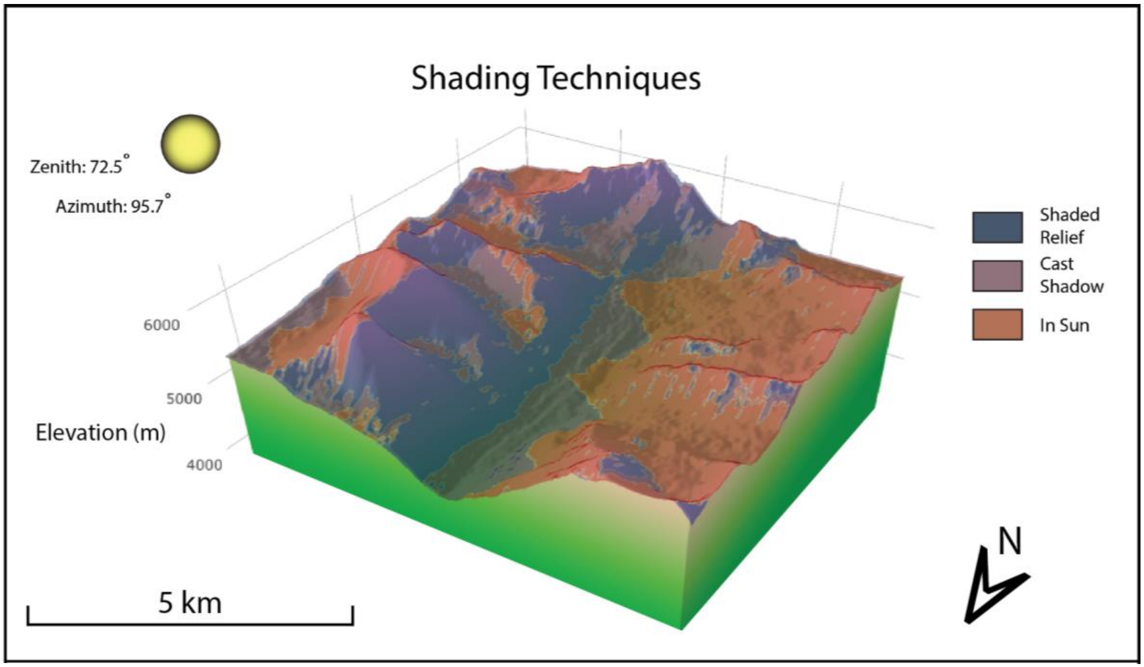

Figure 1. Comparing two different shading methods in the Satluj sub-basin within the Indus watershed. Shading is calculated on April 1, 2013 at 7:33am. Notice the importance of incorporating both methods in order to determine shading in this glacial valley. Both methods, but specifically cast shadows, are most prevalent early in the morning and late in the evenings when the zenith angle is large.

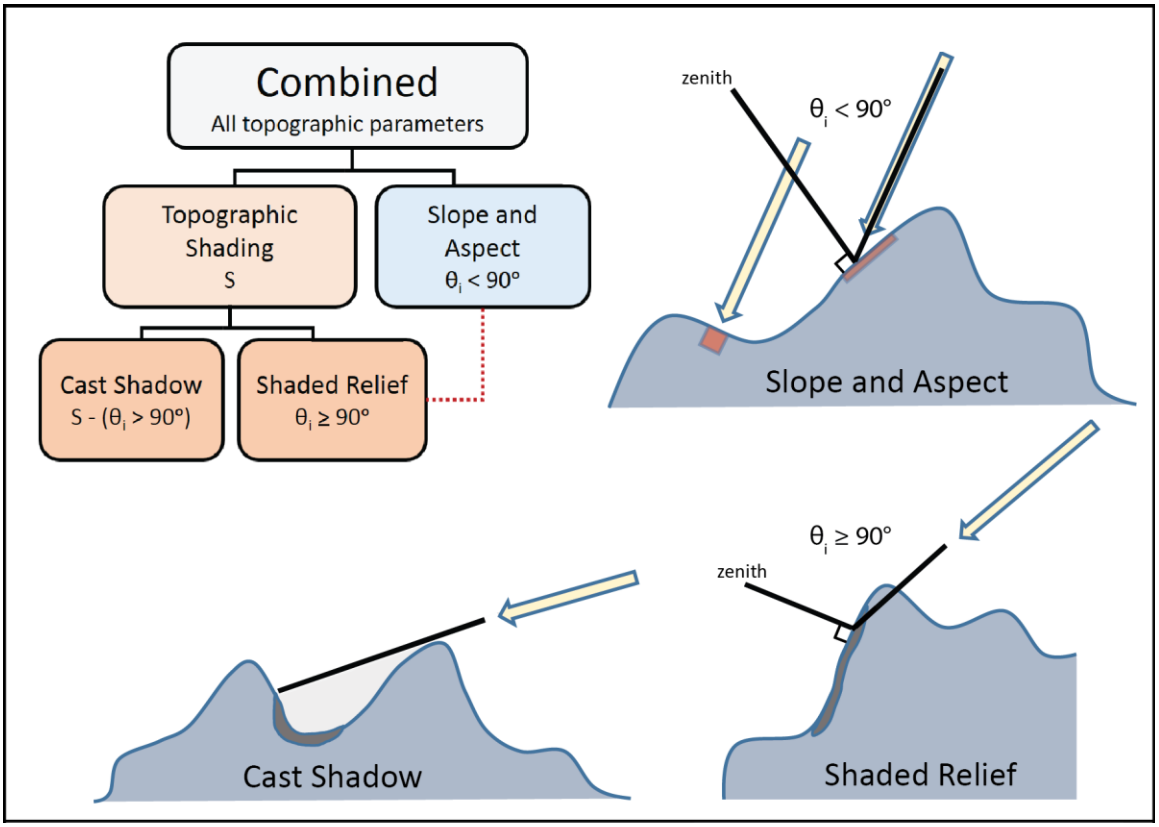

Figure 2. Flowchart depicting the three main topographic parameters of interest: slope and aspect, shaded relief, and cast shadows. Slope and aspect describes the loss in solar radiation due to the angle of incidence (less than 90°). Shaded relief describes self-shadowing due to the slope and aspect at a given point, and occurs once the angle of incidence becomes greater than 90°. Cast shadows occur when shadows are cast from surrounding terrain. Topographic shading is a binary value indicating whether a point is in shade or sun and includes both shaded relief and cast shadows. The combined effect includes the loss in solar radiation due to slope and aspect along with topographic shading.

CHAPTER 2

DATA AND METHODS

In this study, we will use a solar radiation model in conjunction with a topographic model to simulate the distribution of direct solar radiation across glacier surfaces. The models will be used to parse out the change in irradiation due to specific topographic parameters such as slope and aspect, shaded relief, and cast shadows. The key inputs to the models will be information on glacier location and size, and digital elevation models (DEMs).

First, we apply these models to two individual glaciers in HMA. We then apply idealized scenarios to these glaciers in order to test the sensitivity of each to different valley-aspects, and latitudes. Third, we evaluate regional patterns in topographic shading by assessing the variability of each topographic parameter across multiple glacierized basins. We then compare changes in the impact of topographic shading on glacier ice across varying zones of HMA. Finally, we combine our topographic solar radiation models with a modified temperature index model to calculate the change in melt when topographic shading is not incorporated.

2.1 Modeling Solar Radiation

To first order, solar radiation is a function of latitude and day of the year, which can be easily integrated on a daily timescale. However, when considering topographic effects, the position of the sun is required in order to properly calculate the amount of incoming solar radiation. Assuming a flat plane, the solar position is described by a combination of the zenith and azimuth angles. Zenith is defined as a point or line directly above an observer; the zenith angle is the angle between zenith and the position of the sun. Azimuth is the angle along the horizon spanning a total of 360°, zero typically being north. We calculate solar zenith (Z) and azimuth (ϕ) angles as (modified from Iqbal 2012):

$$cosZ = sin\beta sin\delta + cos\beta cos\delta \cos(\omega - \lambda) \qquad (3)$$

$$cos\phi = \frac{sinZ sin\beta - sin\delta}{cosZ cos\beta} \qquad (4)$$

where β is latitude, δ is the solar declination, and (ω-λ) is the hour angle (Appendix). Latitude is given at a location of interest. Solar declination is the latitude of the sub-solar point, which fluctuates between -23.5° and 23.5°. Solar declination is defined as:

$$\delta = 23.45 cos\left(\frac{360(J-172)}{365}\right) \qquad (5)$$

where J is the day of the year. The hour angle is the difference between the solar longitude (ω) and the longitude at which the zenith angle is being calculated (λ). The hour angle is most commonly calculated by using local time, which can be problematic in remote regions such as the Himalaya, which spans multiple time zones with unclear boundaries. Although the hour angle can also be calculated using solar noon at the prime meridian and longitude, we opt for another approach that involves calculating the hour angle at sunrise and sunset. With these values, we can then easily incorporate a consistent time-step throughout the day to calculate solar radiation. Ignoring atmospheric refraction, at sunrise or sunset Z=90° making our cosZ term in equation 3 go to zero. We can then simplify the hour angle at sunrise or sunset to be:

$$(\omega - \lambda)_{sunrise/set} = -\frac{sin\beta sin\delta}{cos\beta cos\delta} = -tan\beta tan\delta \quad (6)$$

This produces two values for $(\omega\text{-}\lambda)_{\text{sunrise/set}}$, symmetrical around the longitude of the observer. Because of atmospheric refraction and the diameter of the sun, sunrise and sunset do not occur at Z=90°, however, the magnitude of difference when these parameters are included is extremely small and will not likely affect our results when calculating the impact of local topography on direct solar radiation. Furthermore, because of limitations in modeling shading, we ignore these added effects. With all three variables accounted for, we are able to solve for the zenith and azimuth angles and can accurately determine the solar position at a given time interval throughout the day. This is essential for determining both shaded relief and cast shadowing.

We model potential clear-sky direct solar radiation, as it passes through the atmosphere, at 15-minute time-intervals throughout the melt season (April 1—September 31). The time-interval is converted into degrees for equation 3 using the conversion of

360° per 24 hours, or 15° per hour. Potential clear-sky direct solar radiation passing through the atmosphere is calculated as:

$$I_a = I_0 \left(\frac{R_m}{R}\right)^2 \psi_a{}^{\frac{P}{P_0 cosZ}} \tag{7}$$

where I_0 is the solar constant (~1368 Wm^{-2}). R is the sun-Earth distance (subscript m refers to mean). ψ_a is atmosphere clear-sky transmissivity (a constant of 0.75 is used – Hock, 1997). P is atmospheric pressure and P_0 is mean atmospheric pressure at sea level. Z is local zenith angle, which accounts for the size of air mass that radiation must travel through before arriving at the surface. Equation 7 has been modified from Hock (1997) to exclude the parameter responsible for attenuation at the surface. This term will be added later in the topographic model. Mean pressure (*P*) is calculated across the glacier surface using a standard barometric formula:

$$P = P_0 \left(1 - \frac{Lh}{T_0}\right)^{\frac{gM}{R_0 L}} \tag{8}$$

where *L* is the standard temperature lapse rate for dry air, *h* is the mean elevation of the glacier, T_0 is the standard temperature at sea level, *M* is the molar mass of dry air, and R_0 is the universal gas constant. With the solar position defined by the zenith and azimuth angles, and potential clear-sky atmospheric solar radiation determined, we can account for topographic effects such as slope, aspect, and shading.

2.2 Topographic Modeling

We create four topographic solar radiation models that work in conjunction with equation 7. Each of these models alters the way in which irradiance is received at the surface. Previously, we calculate the solar zenith angle in equation 3 assuming a flat plane, which is used to calculate solar radiation as it is attenuated through the atmosphere. However, this does not account for variability in solar radiation arriving at the surface. Potential clear-sky solar radiation arriving on an inclined surface is calculated as:

$$I_c = I_a cos\theta_i S \qquad (9)$$

where I_a is potential clear-sky direct solar radiation from equation 7, θ_i is the incident angle, and S is topographic shading, a binary value indicating whether a given cell is in "shade" (0) or "sun" (1). Topographic shading is calculated with a modified ray-tracing algorithm that uses a solar illumination plane perpendicular to the sun's zenith angle in order to determine if a cell is blocked by surrounding cells at a certain zenith and azimuth angle (Corripio, 2003). This method incorporates both shading from relief and cast shadows. The incident angle is the zenith angle modified for a surface with a specific slope and aspect. The incident angle is calculated as:

$$cos\theta_i = \cos Z \cos S + \sin Z \sin S \cos(\phi - E) \qquad (10)$$

where Z is zenith angle from equation 3, ϕ is azimuth from equation 4, and E is exposures, a value between -180 and 180° defined as the slope aspect with respect to a south-facing direction.

Table 1 shows four topographic models that are variations of equation 9 in order to test the sensitivity of incident solar radiation to specific topographic parameters. Model 1 does not account for any topographic parameters. Incident irradiance is calculated on a flat plane, which only incorporates the zenith angle (Z) in place of the incident angle. Model 2 still assumes a flat surface for slope and aspect; however, this model includes topographic shading (S), both from shaded relief and due to surrounding topography. Model 3 incorporates the incident angle (θ_i), which accounts for both slope and aspect at a given pixel. Model 4 is the complete model represented in equation 9, which correctly accounts for the incident angle and topographic shading.

We use these four models to calculate the individual contribution due to three distinct topographic parameters: slope and aspect (incident angle), shaded relief, and cast shadows along with the total shading and all parameters combined (Table 1, Figure 2). Shaded relief is automatically incorporated in the calculation of the incident angle (θ_i), because it relies solely on slope and aspect. If a given pixel has an incident angle greater than 90°, the pixel is shaded by relief; if less than 90°, the pixel is considered to be in sun (Figure 2). Although this shading method alone is used in some topographic analyses, it is incorrect as it does not incorporate cast shadowing from adjacent valley walls. The shading algorithm used to determine S also incorporates shaded relief along with cast shadowing from valley walls. Because shaded relief resides in two terms of equation 9, it is possible to parse out the individual contribution due to cast shadows, which then allows us to determine the amount of shaded relief contributing to the total shading over a given pixel.

2.3 Data

This study utilizes the 30-meter resolution ASTER global digital elevation model (GDEM) to simulate topographic terrain in the models. The ASTER GDEM is easily obtained without void regions and is known to have a greater vertical accuracy and detail over the Shuttle Radar Topography Mission (SRTM) DEM (Arnold et al., 2006). In addition, interpolation techniques for the void-filled SRTM DEM introduce gross errors that degrade the quality of topographic parameters (Frey et al., 2012). Although a 30-meter resolution DEM does not fully capture the actual topographic complexity in a glacial valley, it serves as an adequate representation in order to measure the overall effect of surrounding topography on solar radiation within our theoretical framework. DEM resolution is further considered in the discussion section of this paper.

Glacier boundaries are determined with the latest shapefiles available from the ICIMOD and the Randolph Glacier Inventory 5.0 (Arendt et al., 2015; Bajracharya et al., 2011). Both inventories delineate glacier ice using a variety of techniques to determine glacier boundaries. For topographic analysis, a buffer of 5 km is generated around the glacier shapefiles in order to include all surrounding topography. The ASTER imagery is then masked to the buffered area to simulate topography that may influence the distribution of solar radiation on the glacier surface.

The buffered extent, or distance of topographic features from a glacier surface, appears to be small as changes in received irradiance beyond an extent of 5 km of glacier border showed little to no change. This suggests that, in general, only immediately adjacent relief significantly alters topographic shading around a glaciated area. Additionally, topographic shading was altered by less than 0.01% when changing DEM extent from 5 km to 3 km beyond the Satluj Glacier boundary. Because valley glaciers are constrained by the surrounding topography, only local topography will immediately affect incoming solar radiation. However, at higher glacier elevations, the visible horizon can become much larger, in which case the extent must incorporate topographic features within visibility. For this study, a buffer of 5 km proved to be sufficient.

2.4 Idealized Scenarios and Regional Study

We implement two idealized scenarios in order to test the sensitivity of the shaded relief and cast shadows to changes in overall glacier aspect and latitude. For these scenarios, two glaciers of contrasting topography are selected. The impacts of shaded relief and cast shadows are calculated for each glacier. Then, for the first scenario, each glacier is rotated in each of the remaining three cardinal directions (East, South, and West). This allows us to calculate changes in direct irradiance due to different valley aspects for the two glaciers. The second idealized scenario calculates the relative change in irradiance due to total shading across varying degrees of latitude (20-50°) for the same two glaciers. Thus, in these idealized scenarios, glacier size, slope, and surrounding topography are constant, while aspect and latitude are systematically varied.

Modeling the change in irradiance for a given glacier under idealized scenarios is useful for understanding relative importance of glacier aspect, morphology, and latitude. However, because of the unique nature of local topography, the role of cast shadows can be highly variable even for glaciers of similar aspect, morphology, and latitude. In order to quantify the variability in our idealized scenarios, we also apply our cast shadow model to four glaciated regions across the greater Himalaya (Figure 3). These regions span multiple latitudes and degrees of topographic relief, and include a larger sampling of glacier geometries throughout HMA. Only glaciers larger than 3 km^2 were used in the analysis in order to exclude small cirque glaciers, and focus on valley glaciers with a developed tongue. These glaciers are then separated based on general valley-aspect of the ablation zone (lower half of the glacier below mid-elevation), as we are most concerned with the cast shadowing effect from the narrow valley walls along these lower elevations. The valley aspect for each glacier is determined based on the mode of pixels of a reclassified aspect value. They are then grouped into two categories: North/South and East/West. Glaciers with less than 10% majority aspect are manually corrected and labeled according to the best perceived aspect. A single mean value is calculated across the defined ablation zone of each glacier. This introduces some variability as glacier aspect and morphology can be extremely irregular throughout the lower elevation for these HMA glaciers. For this reason, we include a large sample of valley glaciers for each region, ranging from 80 to 117. A kernel density estimation is fit to the mean values in each region for both North/South and East/West glaciers in order to see how the distribution of each group varies from one another.

2.5 Melt Model

Once we have determined the impact of topographic shading on direct solar radiation, we then test how shading influences actual melt rates on a glacier surface. Although glacial melt is determined by the energy balance at the surface, in situ energy balance data are sparse and typically short term. Additionally, they lack the spatial coverage to perform large-scale regional analyses. Temperature-index models have proven to be useful alternatives for estimating melt (Hock, 1999), and are particularly useful in data-sparse regions such as HMA. We use a modified temperature-index model in order to quantify the effect of topographic shading on glacier melt. This model includes the addition of a solar radiation term, which allows for better accuracy in estimating melt on a diurnal timescale (Hock, 1999). We solve for melt in 15-minute increments throughout the melt season (April 1—September 31, 2013). Melt is calculated as:

$$M = \begin{cases} \left(M_F + \propto_{snow,ice} I\right) T, & T > 0 \\ 0, & T \leq 0 \end{cases} \tag{11}$$

where M_F is the hourly melt factor (mm h^{-1} °C^{-1}), α is the radiation factor for a snow- or ice-covered surface (mm m^2 h^{-1} W^{-1} °C^{-1}) and is included to account for surface differences between the two, I is the potential clear sky direct solar radiation calculated in equation 9 (Wm^{-2}), and T is air temperature (°C). We use a melt factor of 0.11 mm h^{-1} °C^{-1} for this model. Hock et al. (1997) empirically derived radiation coefficient (α) values of 1.6e-3 and 1.8e-3 for snow covered and ice surfaces, respectively. Because we are interested in testing the magnitude of melt to first order, we use an intermediate value of 1.75e-3 for our radiation coefficient, rather than distinguish between snow and ice. Temperature data from 2013 are obtained through the High Asia Refined analysis (HAR), and was chosen due to the high spatial and temporal resolution. 2013 is the latest year of data provided by HAR. A global standard lapse rate of -6.5°C/km is applied over the glacier surface.

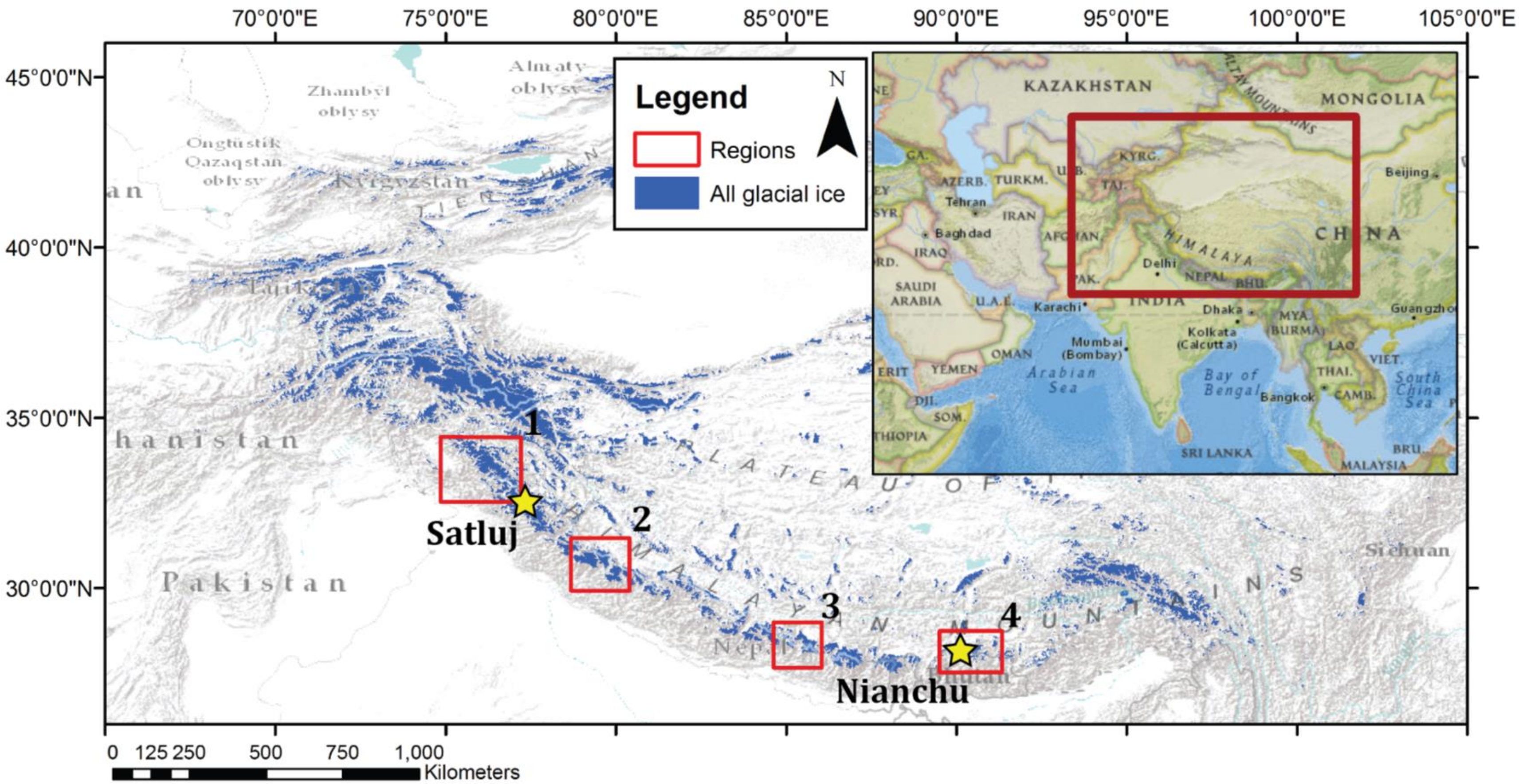

Figure 3. High Mountain Asia, showing glacier ice in blue. Two selected glaciers of interest are shown as yellow stars. Four red boxes indicate the areas selected for the regional analysis. Regions incorporate the Jammu Kashmir, Himarchal Pradesh, Everest, and Bhutan regions. Sources: Arendt et al., 2015, National Geographic, Esri, DeLorme, HERE, UNEP-WCMC, TomTom, Intermap, increment p Corp., GEBCO, USGS, NASA, ESA, METI, FAO, NPS, NRCAN, NOAA, iPC, GeoBase, IGN, Kadaster NL, Ordinance Survey, Esri Japan, Esri China (Hong Kong).

Table 1. Topographic Solar Radiation Models	
Model 1 (flat + no shade)	$I_a \cdot \cos Z$
Model 2 (flat + all shade)	$I_a \cdot \cos Z \cdot S$
Model 3 (slope + shaded relief)	$I_a \cdot \cos\theta_i$
Model 4 (slope + all shade)	$I_a \cdot \cos\theta_i \cdot S$
Slope & Aspect	Model 4 − Model 2
Total Shading	Model 2 − Model 1
Cast Shadow	Model 4 − Model 3
Shaded Relief	Total Shading − Cast Shadow
Combined	Model 4 − Model 1

CHAPTER 3

RESULTS AND DISCUSSION

Besides latitude and Julian day, local topography and glacier geometry chiefly determine the amount of potential clear-sky solar irradiance received at the glacier surface. Although glaciated basins likely show an overall regional similarity, local valley topography and geomorphology can be dramatically different. As such, the influence of topographic parameters on modeled solar irradiance is expected to be highly variable between glaciated valleys, as well as spatially heterogeneous across a single glacier.

3.1 Topographic Impacts on Individual Glaciers

For the first run of our topographic solar radiation models, we selected glacier GLIMS Id G077860E31914N found in the Panjnad basin of the Indus watershed in the Himarchal Praedesh region of the western Himalaya. We refer to this glacier hereafter as the Satluj Glacier, due to the sub-basin in which it resides. We chose this valley glacier because it has a clear north-facing aspect, a well-developed glacier tongue, and its location is in an area of steep topography and high relief. Additional information can be found in Table 2.

We calculate mean change in irradiance due to different topographic parameters from daily mean values throughout the summer melt season (April 1—September 31). Figure 4 shows a smoothing spline of the mean change in irradiance due to each topographic parameter and their totals across elevation for the Satluj Glacier. The spatial variability across the glacier surface is also included for visual aid (Figure 4a-d). The mean change in irradiance across increasing elevation for all combined topographic parameters is greatest at the lowest elevations (< 4800m) and higher elevations (5600m). Slope and aspect tend to play an important role across all elevations but become more significant as elevation increases. The effects of shaded relief also increase with increasing elevation. In contrast, we see a decrease in cast shadowing with increasing elevation. Cast shadowing only plays a significant role where the surrounding terrain is steep, close in proximity, and large enough to cast a significant shadow over the valley. For this particular glacier, this occurs at the lower elevations of the ablation zone.

In Figure 4, the Satluj Glacier can be separated into two main zones across elevation. Change in irradiance on glacier ice less than 5050m is dominated by cast shadowing, while change in irradiance on ice greater than 5050m appears to be more controlled by slope and aspect. This cross-over point in elevation marks the boundary at which the Satluj becomes constrained to the valley. Above 5050m, the glacier cirque spreads out to incorporate various aspects. These new aspects receive more direct solar radiation than their north-facing counterparts (Figure 4c-d). Additionally, the mean change in irradiance from cast shadowing significantly decreases in both the east- and west-facing direction, but not on the south-facing tributary (Figure 4b - right side).

Comparing the overall mean change in irradiance from shaded relief and cast shadowing for the Satluj Glacier, topographic shading is dominated by cast shadows, particularly at lower elevations along the ablation zone. This is critical, as changes in net shortwave radiation in the ablation zone (e.g., where the energy budget is frequently already positive) will have a larger effect on glacier mass balance than changes in the accumulation zone (e.g., where the energy budget is usually negative enough that a small increase in incoming energy likely won't result in significant melt). Furthermore, Figure 4 shows that the influence of topographic shading is also more significant than the mean change in irradiance from slope and aspect throughout the ablation zone. However, this is not true when comparing the effects of slope and aspect with shaded relief alone. These results emphasize the importance of correctly incorporating both methods of topographic shading when modeling solar radiation or surface energy balance, particularly for north-facing valley glaciers in areas of high relief.

We select another north-facing valley glacier, located in the eastern Himalaya on the China-Bhutan border (Table 2). The Nianchu Glacier (GLIMS Id G090036E28191N) spans a slightly higher range of elevation and is surrounded by less topographic relief than the Satluj Glacier. We also refer to this glacier as its sub-basin name for convenience. Figure 5 shows an overall increasing mean change in irradiance from combined topographic parameters with increasing elevation for the Nianchu. Both shaded relief and slope and aspect follow a similar trend of increasing mean change in irradiance with elevation. Cast shadowing tends to have only a slightly larger effect than slope and aspect at elevations below 5500m.

The lower impact from cast shadows on the lower elevations for the Nianchu is due to lower relief from the surrounding valley walls alongside the glacier toe, as well as the slight northeastern direction of the valley. Sunrise occurs further northeast during the summer months than during the rest of the year, and if the valley faces this direction and is surrounded by lower relief, the effect from cast shadowing can be minimal. Once above 5500m, cast shadowing increases dramatically (Figure 5), then gradually decreases again at higher elevations. This shadowing can be seen in Figure 5b, at the point in which the glacier divides into two tributaries and becomes more north facing. Although the Nianchu Glacier shows how variable topographic shading can be, shading is still a significant influence on the overall mean change in irradiance at the surface, even surpassing the impact of slope and aspect at certain elevations.

Figure 6 shows the hypsometry of the Satluj and Nianchu Glaciers, with a bin size of 30 meters. The colors indicate the mean change in irradiance for each elevation bin. The Nianchu is more than twice the size of the Satluj Glacier, and is found at higher elevations. The elevational distribution of Satluj Glacier is close to normally distributed around the mean elevation, while the Nianchu is somewhat right skewed, with a much larger bulk area at lower elevations. This may be due to the extremely low slope angle of the glacial toe. Areas that receive the highest effect from shading are directly north-facing aspects surrounded by high relief. This occurs on the toe of the Satluj Glacier, and across the mid-elevations for the Nianchu.

Topographic shading occurs when high zenith angles cause shadows to be cast from surrounding topography or when steep slope angles cause surrounding relief to block solar rays. As such, the impact can be slight over the course of small timescales. However, our results show that the influence of topographic shading can become extremely meaningful when integrated over the course of the entire melt season.

Additionally, because topography is highly variable and differs significantly from one basin to the next, the effects of topographic shading are equally heterogeneous.

3.2 Idealized Scenarios and Regional Comparison

3.2.1 Idealized Scenarios

In order to quantify how sensitive topographic shading is to parameters such as valley-aspect and latitude, we perform idealized scenarios on the Satluj and Nianchu Glaciers. For aspect sensitivity, each glacier is rotated in the three remaining cardinal directions, east, south, and west.

For the Satluj, shaded relief only slightly changes across increasing elevation (Figure 7) when the glacier is rotated to east, south, and west facing. Cast shadows, on the other hand, show significant differences for north- and south-valley aspects as compared to east- and west-valley aspects. For the north and south directions, we see the largest mean change in irradiance at the lower elevations. This makes intuitive sense as shading is most important when the zenith angle is high, which occurs when the sun is rising in the east and setting in the west. East- and west-valley aspects lose the steep, adjacent topography that is able to cast significant shadows in high zenith angles. However, we see an increase in the mean change in irradiance in the upper elevations for east and west aspects, as the upper tributaries are now facing north and south (Figure 4).

The Nianchu Glacier shows a less clear pattern in aspect sensitivity; however, some differences are notable. Cast shadowing appears to be most significant for lower and mid-elevations on north- and south-valley aspects (Figure 7). Additionally the upper elevations for the south direction show a large increase in cast shadows. Shaded relief also shows a larger mean change in upper elevations for north and south directions. One interesting point when comparing both glaciers side-by-side is that the impact of shaded relief only surpasses cast shadowing in the north-facing direction.

In general, we see that shading is more significant on north- and south-valley glaciers, particularly in the lower elevations of valley glaciers. This is a particularly important result for regions like the Himalayas where valley glaciers are dominantly north- or south-facing. Although we continue to see variability in shading, this can be a useful proxy to determine how impactful shading might be on a given glacier.

We also take these same two, north-facing glaciers and move them across different latitudes in order to test the sensitivity of shading with respect to latitude. Figure 8 shows an overall relative decrease in mean irradiance with increasing degree of latitude for both the Satluj and Nianchu Glaciers. The trend of relative change in mean irradiance for each glacier closely follows a simple mathematical trend of one minus the tangent of the change in degree latitude (β). Cast shadows become larger with increasing zenith angles, and the zenith angle will increase proportional to latitude (see Appendix). This simple mathematical trend over-predicts for the Satluj, and under-predicts for the Nianchu. This may be due to the fact that lower elevations on the Satluj are surrounded by steeper topography.

3.2.2 Regional Analysis

In addition to the idealized scenarios, we model the variability in irradiance on a regional scale. Initially, we apply the models to the full Satluj basin including the surrounding glacial valleys (Figure 9). This expanded view offers a variety of valley aspects and different morphologies. Shaded relief (Figure 9a) appears to be significant only on extremely steep terrain that is not south facing. Although this may be a significant topographic parameter in the upper cirques of some glaciers, the impact is minimal in glacier valleys. Cast shadows (Figure 9b) are most pronounced in low-elevation north- and south-facing valleys, as predicted in our aspect sensitivity tests. Although the mean change in irradiance increases due to slope and aspect for some south-facing valleys (Figure 9c), this effect is offset, and in some cases overwhelmed, by cast shadows (Figure 9d). By calculating the influence of these topographic parameters on a larger scale, we are able to confirm the results from our aspect sensitivity analysis (Figure 7). We also see clear patterns for each parameter across a much larger region.

Additionally, four regions across the greater Himalaya were selected in order to quantify the impact of topographic shading both within each selected region as well as between regions (Figure 3). This allows us to distinguish patterns while incorporating more topographic variability.

In each region, we see that North/South-facing glaciers are more impacted by cast shadowing (Figure 10). Additionally, we see that the peak values in our North/South distributions (mode) show a greater change in regions of higher latitude and relief (Regions 1 and 2), fluctuating from -28.7 Wm^{-2} in the highest latitude to -20.7 Wm^{-2} in the lowest. Our regional model validates the findings in our idealized scenarios, suggesting that the impact of shading is most prominent on north- and south-facing valleys. We also see a shift of mean change in irradiance between regions, showing a general increase of the effect of shading in regions located at higher latitudes.

Additional improvements to the regional analysis will allow us to explore more patterns between HMA glaciers and topographic shading. In particular, improved methods permitting us to better distinguish between valley aspect for a given glacier are also needed in order to make a more robust comparison.

Outside of latitude, topographic shading is mostly controlled by the distance, direction, and size of the immediate surrounding topography, making it very difficult to predict without some metric to incorporate local basin morphology. Although aspect and latitude alone cannot serve as parameterizations, they play a significant role in contributing to the influence of topographic shading on a glacier surface.

3.3 A Modified Temperature-Index Model

The results above demonstrate that topographic shading can significantly alter potential incoming direct solar radiation throughout the melt season (Figures 4, 5). Cast shadowing, which appears to be the dominant component of shading for some glaciers and the most-often neglected parameter, generally only occurs for a short amount of time in the early hours of the morning, and late hours of the evening—especially in the ablation area of a valley glacier. During these hours, the air temperature is cold, and the melt potential on a glacier surface is low. In order to test the impact topographic shading has on glacier melt, we run a modified temperature-index model that incorporates potential direct clear-sky solar radiation.

Our temperature-index model shows melt as high as 8m in the lowest elevations on the ablation zone (Figure 11). When shading is removed, an additional 0.5 to 0.8

m.w.e of melt occurs on the lowest portion of the ablation zone. This is a significant contribution over the course of a single melt season, as it indicates a 5-10% increase to overall melt on the glacier toe.

Under current trends of increasing global temperature, we can presume that the Satluj Glacier will continue to recede up-valley. However, this response may be reduced somewhat by the decrease in melt due to shading (Figure 11). Ultimately, once the glacier tongue has receded beyond the most-shaded region in the valley (Figure 4), melt will further enhance throughout the ablation zone, as the reduction in shortwave radiation due to shading will be minimized. This would also be relevant for the Nianchu Glacier. Once the glacier has retreated into the mid-elevations, where shading is very pronounced, melt rates over the ablation zone would likely decrease. This suggests that shading may not only be a useful tool for improving our understanding of the mass balance of valley glaciers throughout HMA, but will likely improve our understanding of the magnitude and rate of response of glaciers to climatic change.

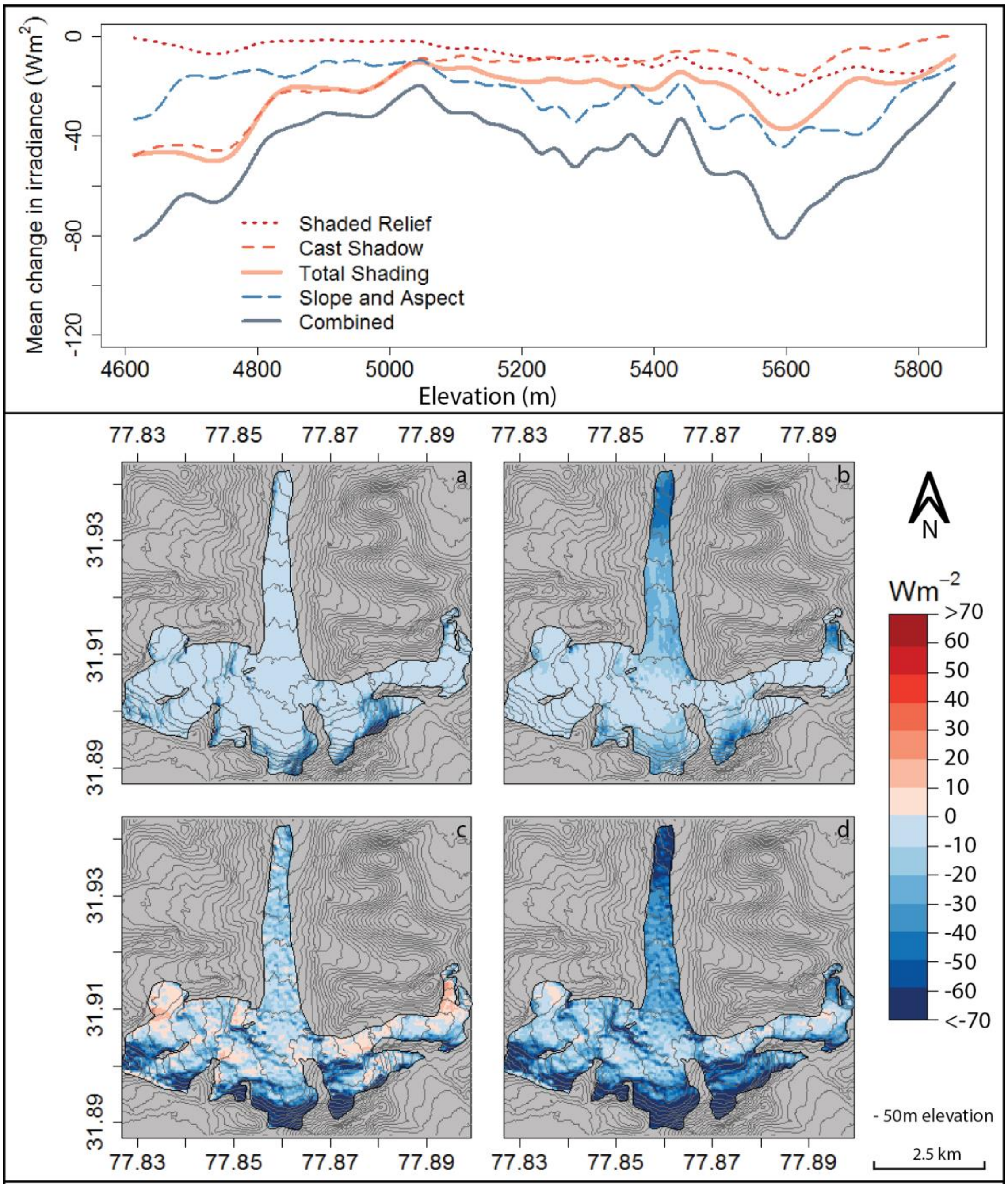

Figure 4. Satluj Glacier. Mean change in irradiance throughout the summer melt season due to shaded relief (a), cast shadowing (b), slope and aspect (c), and combined topographic parameters (d). A smoothing spline was fit to the irradiance change values along the elevation profile of the glacier. The effect of cast shadowing shows to be more significant than that of shaded relief and slope and aspect at lower elevations where ablation dominates during the melt season.

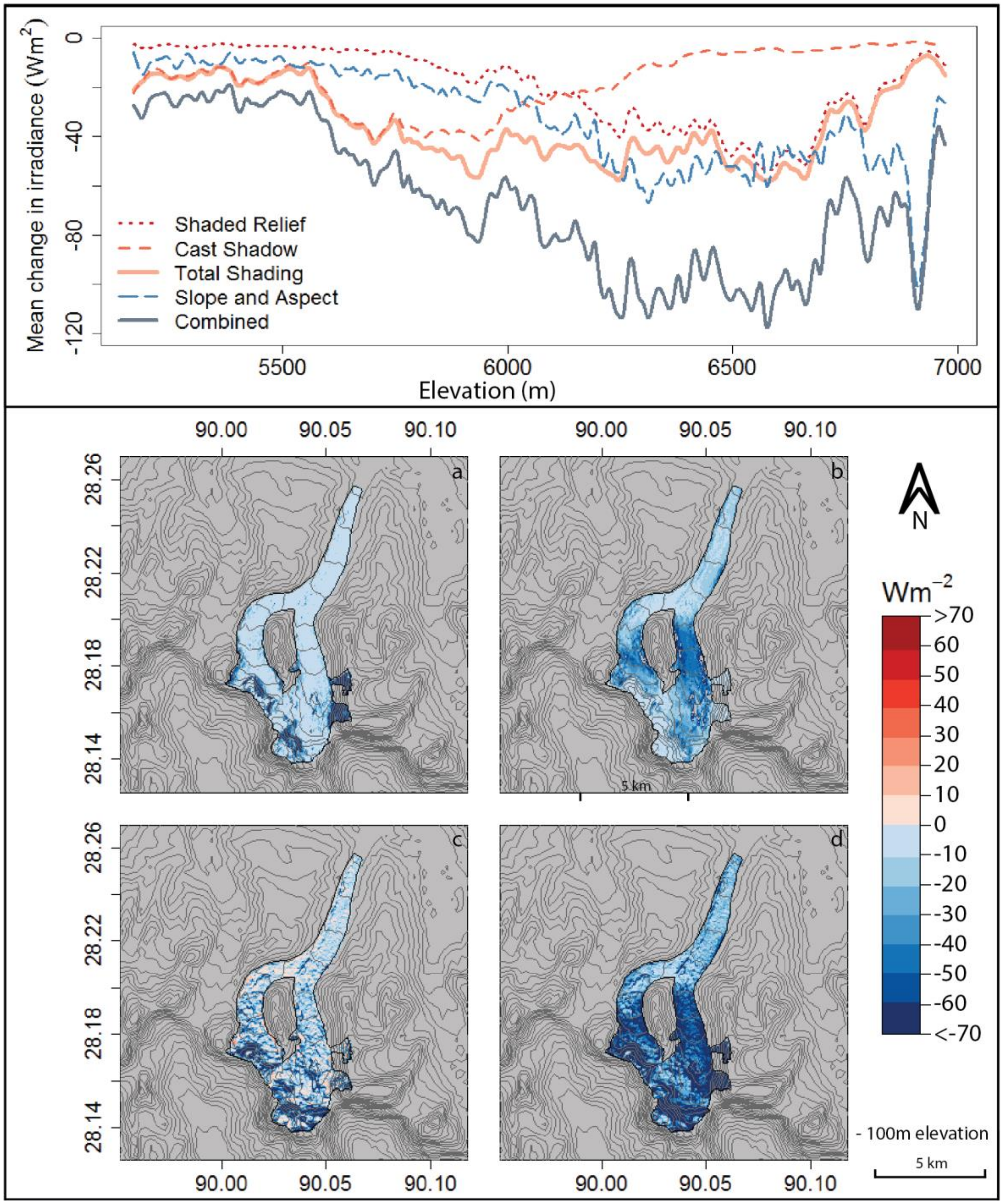

Figure 5. Nianchu Glacier. Mean change in irradiance throughout the summer melt season due to shaded relief (a), cast shadowing (b), slope and aspect (c), and combined topographic parameters (d). A smoothing spline was fit to the irradiance change values along the elevation profile of the glacier. The effect of cast shadowing is largest at mid elevations and occurs once the Nianchu becomes more directly north-facing and is constricted between steep valley walls.

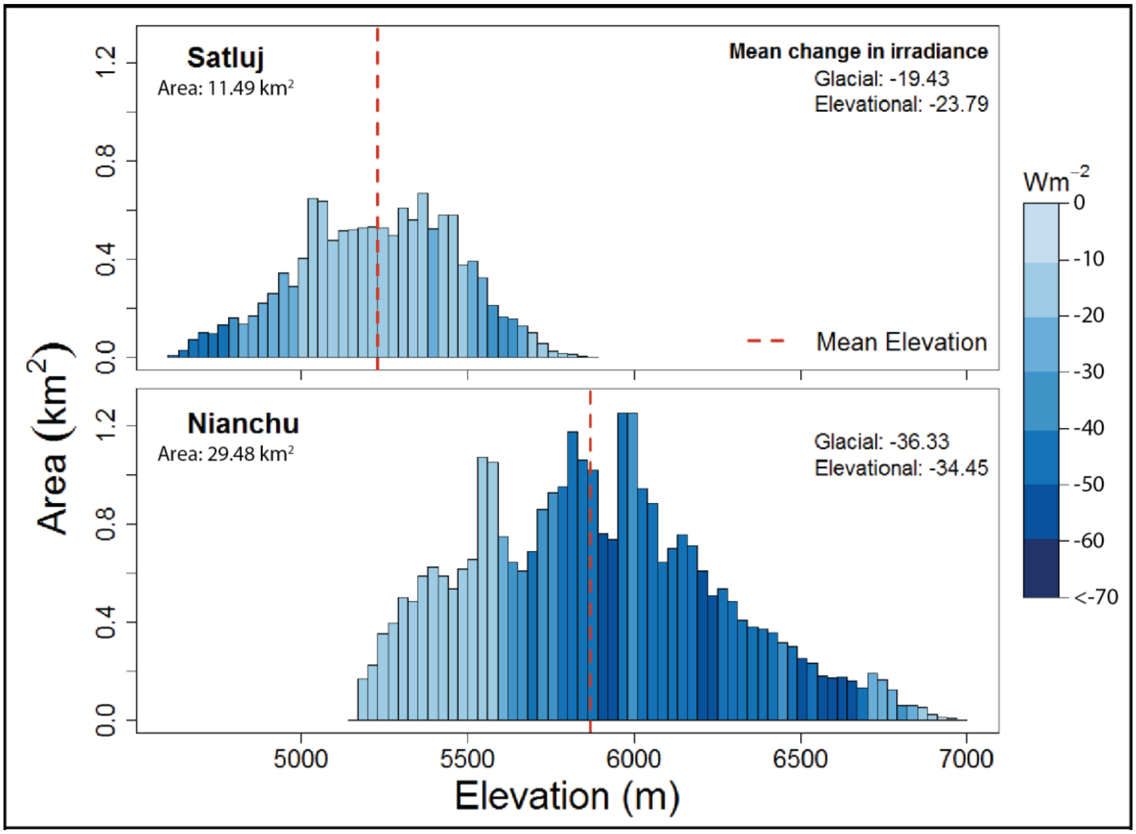

Figure 6. Glacier hypsometries for the Satluj and Nianchu Glaciers. Bin size is 30 meters. Hypsometries are overlain with the mean change in irradiance due to topographic shading across each 30m elevation band. This allows us to compare the amount of area most affected by shading for each glacier. Glacial means take the mean of all pixel values while elevational means take the mean value across all elevation bands. Additional information for each glacier can be found in Table 2.

Figure 7. Idealized scenarios for the Satluj and Nianchu Glaciers. Mean change in irradiance throughout the summer melt season due to shaded relief and cast shadows. Glaciers have been rotated in the four main cardinal directions to observe how shading changes with differing valley aspect. The difference between shaded relief and cast shadows is largest at lower and mid-elevations for the north and south valley direction. Also note that shaded relief is only greater than cast shadowing in the upper elevations of the north-facing direction for both glaciers.

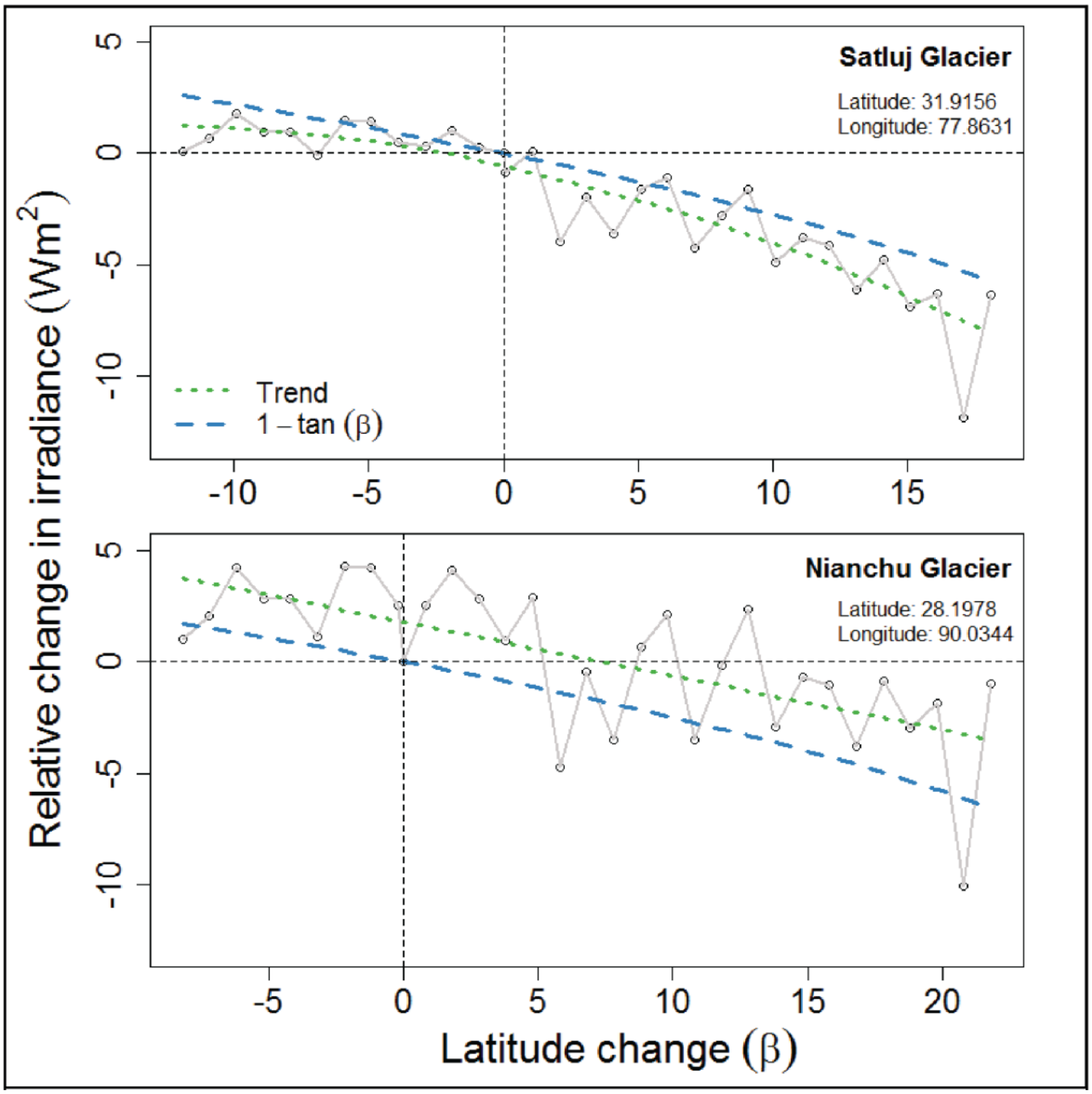

Figure 8. Idealized scenarios for the Satluj and Nianchu Glaciers. Relative change in mean irradiance due to topographic shading as glacier is moved up and down in latitude., both spanning latitude from 20-50°. Mean values are connected (grey) to show stochasticty. The overall trend (green dotted) shows that the effects of shading increase with increasing latitude (β). The relative change mirrors the function 1-tan(β) (blue dashed) which underestimates the relative change for the Satluj, and overestimates for the Nianchu Glacier.

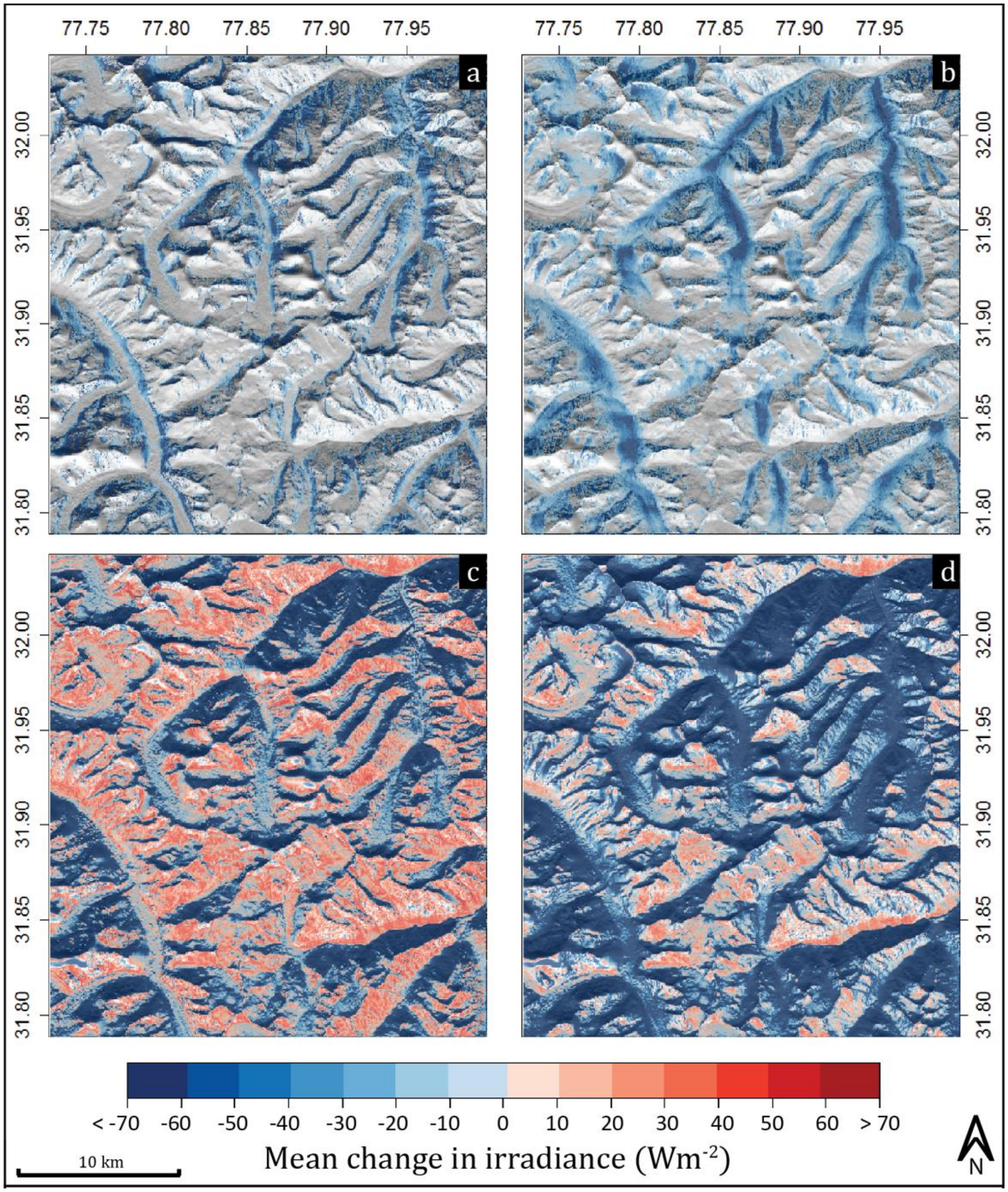

Figure 9. Expanded view of the Satluj Basin including surrounding glacial valleys of various orientation and aspect. Mean change in irradiance due to shaded relief (a), cast shadows (b), slope and aspect (c), and combined topographic parameters (d) are compared. Cast shadows show to be most influential in north- and south-facing valleys and can even offset the increase in irradiance due to slope and aspect for some south-facing valleys. Changes less than ±10 Wm^{-2} are not shown.

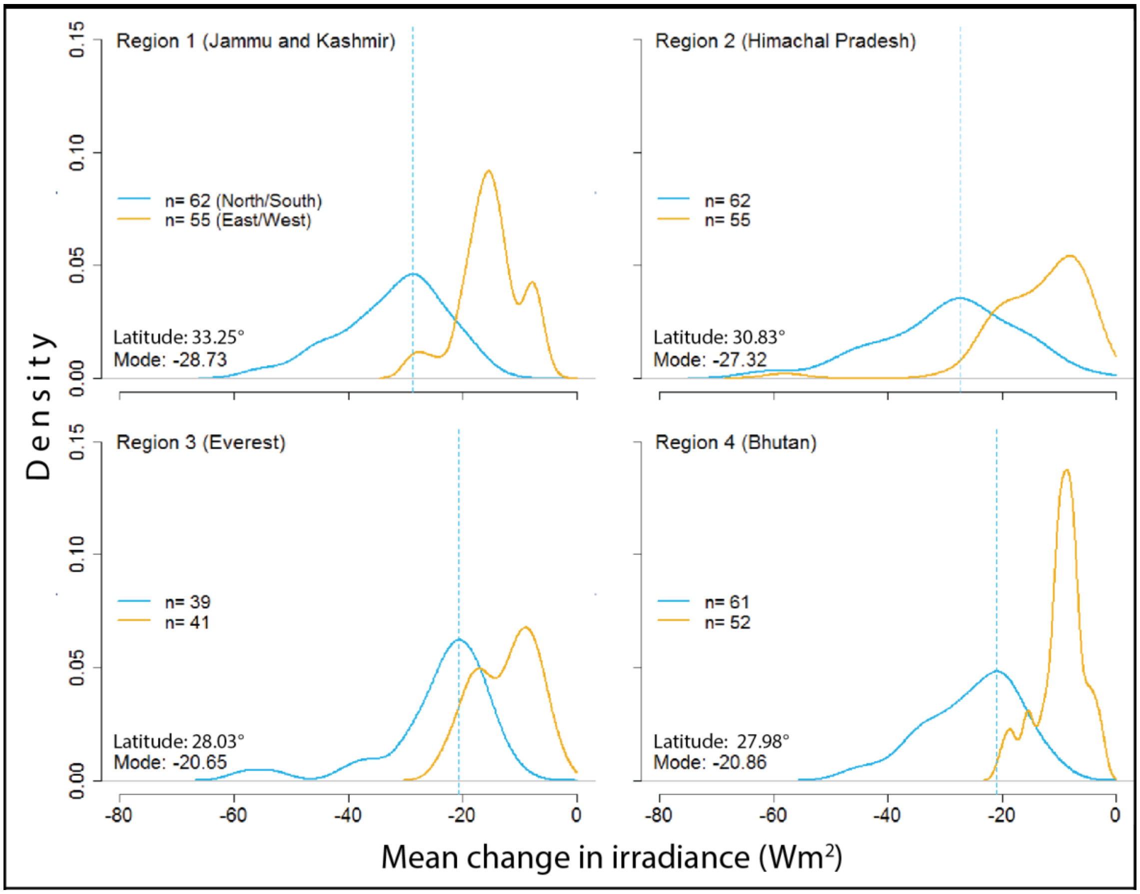

Figure 10. Regional analysis spanning glaciated basins throughout the greater Himalaya of HMA. A mean value for change in irradiance due to cast shadowing is calculated for the ablation zone of each glacier within each region. We see that the distribution for North/South glaciers are more impacted by cast shadowing than East/West glaciers. Only values below mean glacier elevation were used to calculate the mean change for each glacier. Additionally, we see that the peak value for mean change in irradiance is greater in regions of higher latitudes (Regions 1 and 2).

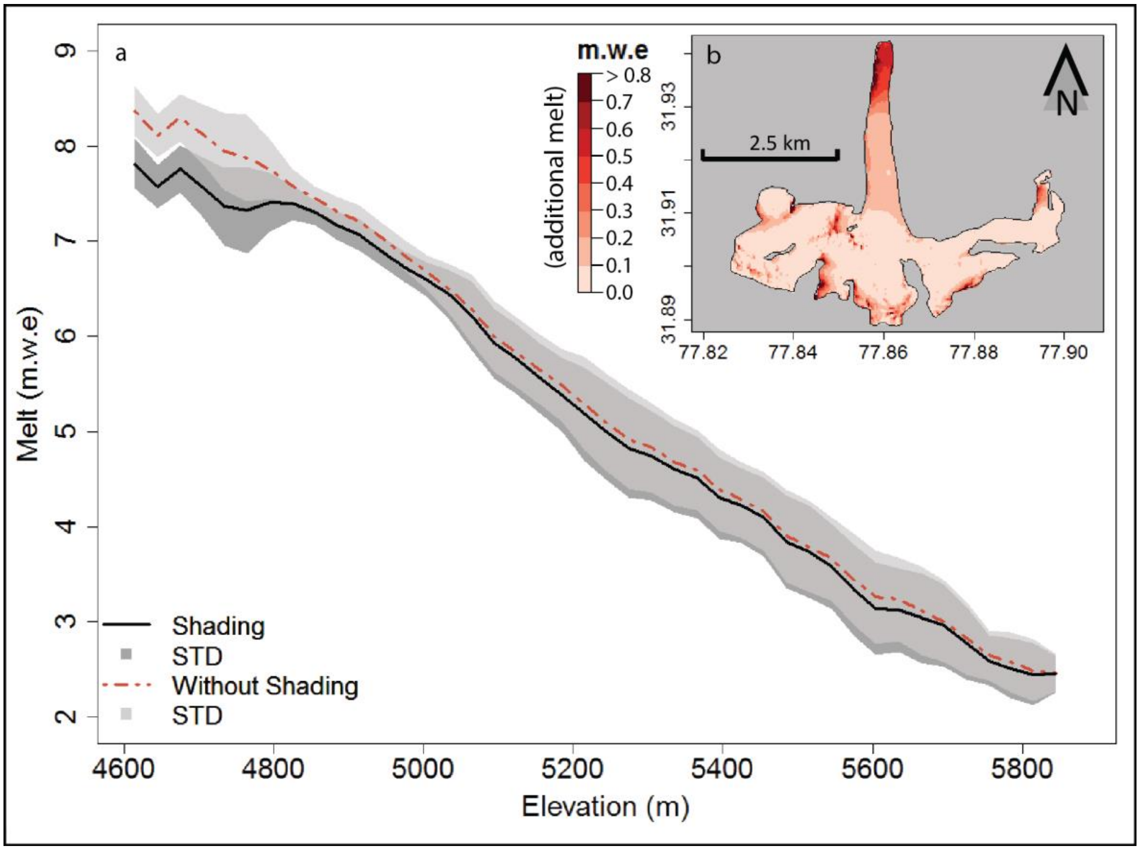

Figure 11. A degree-day model incorporating solar radiation (Hock, 1997) from April 1-September 31, 2013 for the Satluj Glacier. (a) The mean melt across 30 meter elevation bands significantly increases when shading is removed (red dashed), particularly in the lower elevations. One standard deviation of pixel values at the lowest elevations are also statistically different. (b) Melt from 0.5 to upwards of 0.8 m.w.e. occurs on the glacier tounge where shading is significant and temperatures are warmer.

Table 2. Valley Glaciers	**Satluj**	**Nianchu**
GLIMS Id	G077860E31914N	G090036E28191N
Watershed	Indus	Brahmaputra
Basin	Panjnad	Yarlung Zangbo
Latitude°	31.913	28.19
Longitude °	77.86	90.036
Elevation m (min, mean, max)	4617, 5228, 5840	5181, 5869, 6786
Slope ° (min, mean, max)	1, 14, 53	0, 13, 65
Area (km^2)	11.5	29.5

CHAPTER 4

LIMITATIONS AND FUTURE WORK

The results of our topographic shading model highlight the important role of topography on the direct clear sky solar radiation. However, the results are limited by factors related to the DEM resolution and the accuracy of the glacier shapefiles. In addition, the results motivate further work that needs to be done to place topographic shading into context of other components of glacier energy balance.

4.1 Glacier Shapefiles and DEMs

One challenge in accurately quantifying the impact of topographic shading is dealing with inaccuracies in the upper regions of the ICIMOD glacier shapefiles. Some instances showed overlap with the glacier boundary and surrounding ridgelines, which caused error when calculating shading in the upper-most glacier elevations. Improving the accuracy of glacier areas would improve our understanding of topographic shading on glacier surfaces.

The resolution of the digital elevation model is also a concern as topographic features are lost with decreasing resolution. ASTER GDEM, used in this study, builds surface elevation models using orthorectification of two ASTER images, producing a product near 30 m resolution. Although ASTER provides higher detail and better elevation accuracy than other platforms, orthorectification tends to fail in completely snow-covered regions as orthoimages become difficult to align. This, along with the resolution, introduces some inaccuracy as peaks and ridgeline features are smoothed, which lowers effects of shading from topographic features (Arnold et al., 2006).

Hopkins (2010) found a linear increase in glacier melt as DEM resolution decreases from 1 to 1000 m. This is due to decreased textural relief as DEM resolution is reduced. In certain scenarios, Hopkins found that total melt increased with DEM resolution by 4%; however, this value only includes shaded relief and not shading due to adjacent topography. In order to investigate the impact of DEM resolution on cast-shadowing, we take our topographic solar radiation model and decrease the ASTER GDEM resolution. This is done by aggregating nearby cells and generating a new mean value, which decreases the number of cells across the DEM by a factor of two for the first seven model runs, and a factor of four for the last two model runs. Figure 12 shows a decrease in accurately calculating topographic shading as resolution declines for the Satluj and Nianchu Glaciers.

Topographic shading, particularly from cast shadowing, relies on the ability to simulate a change in energy based on detailed features of the surrounding topography. As detail degrades, so does the true effect of topographic shading.

4.2 Diffuse and Terrain-Reflected Radiation

Although we focus specifically on direct solar radiation in this study, we should also consider the impact of the other global radiation terms. While surrounding topography decreases the amount of direct clear-sky irradiance (I) received at the surface, diffuse sky radiation (D_s) and reflected radiation from surrounding terrain (D_t), are also able to alter the net global radiation (Equation 2). A "sky-view" factor (F_s) is necessary to account for both D_s and D_t irradiance at any given point on a glacier surface. Dozier et al. (1990) created a simple approach to approximate sky-view factor for a certain cell based on slope, which has been incorporated into many radiation models (Aguilar et al., 2010; Chen et al., 2013; Kumar et al., 1997). However, the accuracy of this approximation for F_s has not been determined in areas of high relief such as the Himalaya. Arnold et al. (2006) calculates the total diffuse radiation as:

$$Q_{dif} = F_s D_s + D_t \tag{12}$$

where reflected radiation from surrounding topography (D_t) is calculated as:

$$D_t = \alpha_t (1 - F_s) Q_{global} \tag{13}$$

where α_t is the mean albedo of the surrounding terrain, F_s is the sky-view factor, and Q_{global} is measured global radiation. From Equations 12 and 13, it is apparent that D_s and D_t have an inverse relationship with F_s, which is directly related to surrounding topography. As such, we would expect the effects of D_s and D_t to somewhat offset one another in the presence of topography. In Equation 2, direct solar radiation (I) decreases in the presence of higher topography; so D_s will also decrease as F_s decreases, and D_t will increase the radiation received at the surface.

One study found that terrain-reflected irradiance contributes an average of 17% of global radiation for some partially snow-covered sites in the Sierra Nevada (Dozier et al., 1980). However, it is important to note that both diffuse sky and terrain-reflected irradiance is anisotropic and can greatly vary based on the surrounding terrain. Many studies show the importance of including anisotropy for incoming sky and terrain-reflected radiation (Duguay et al., 1993; Gueymard, 1987).

Depending on the orientation of topography, local meteorological conditions, and the mean albedo of the surrounding terrain, D_t could significantly offset the effects of topographic shading on global radiation received on a glacier surface. The relationship between direct, diffuse sky, and terrain-reflected radiation should be further investigated, especially for HMA glaciers.

4.3 Energy Balance

Our topographic model demonstrates how topographic shading influences the shortwave component of energy balance (S_{net}) in regions of HMA. We find that melt can significantly decrease in the ablation zone when correctly accounting for topographic shading on a glacier surface (Figure 11). However, some studies suggest that the decrease in net radiation from less solar radiation on shaded, inclined slopes, is offset by incoming longwave radiation from surrounding terrain (Pluss, 1997). In addition, changes in the radiation budgets will directly impact the turbulent heat fluxes as well. Thus, topography can influence the longwave radiation and turbulent heat fluxes in addition to the shortwave radiation. Future studies should explore the relationship between topographic shading and other energy fluxes (Equation 1).

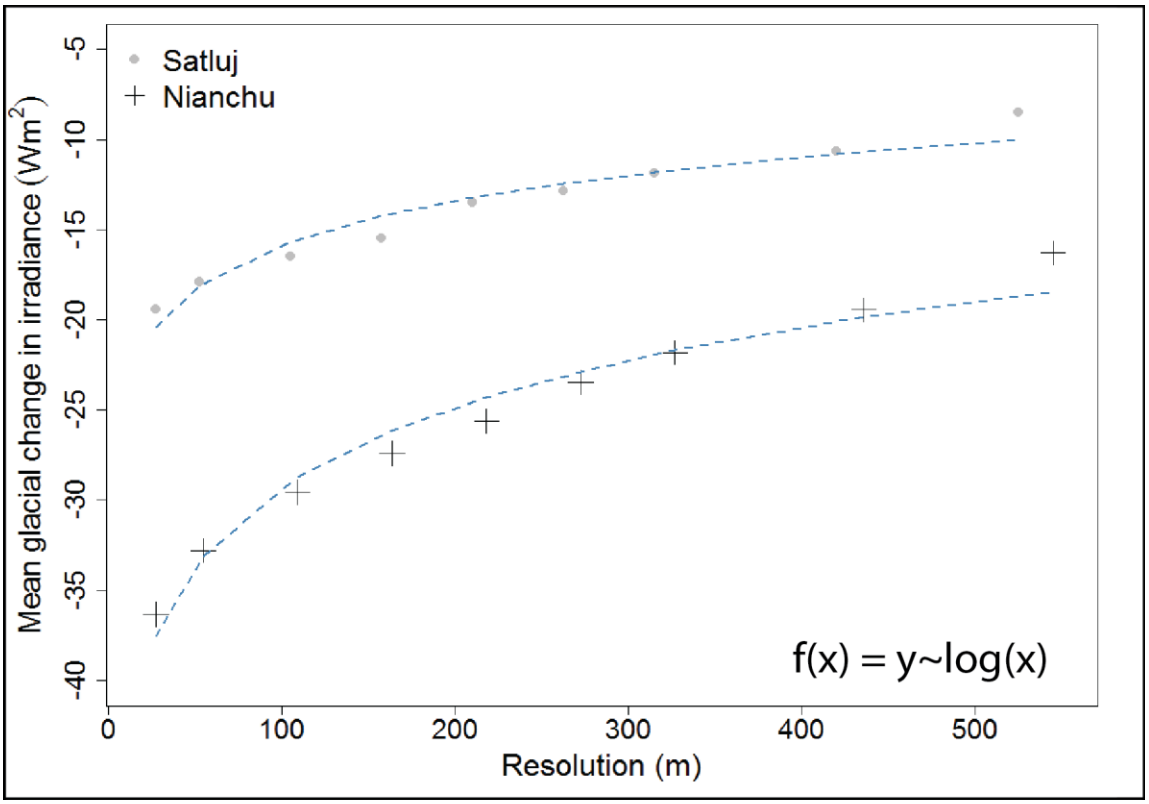

Figure 12. Showing the effect of decreasing resolution on the change in irradiance due to topographic shading for the Satluj and Nianchu Glaciers. Mean change in irradiance appears to decrease with the natural log of resolution. This is due to smoothing topography.

CHAPTER 5

CONCLUSION

Topographic shading is comprised of two components: shaded relief, and cast shadows. Shaded relief is due to slope and aspect and occurs when a surface is blocked from the sun's rays due to its own relief. Cast shadows occur when solar rays project shadows from one topographic feature onto another, which occurs commonly in valleys surrounded by steep valley walls.

We create a topographic solar radiation model in order to quantify the effects of topographic shading. We find that potential direct clear-sky solar radiation can be significantly affected by shading in regions of steep topography and high relief such as HMA. Additionally, we see that cast shadowing can account for a significant decrease in irradiance in the ablation zone. Of the two shading components, cast shadowing appears to be the dominant mechanism contributing to total shading for most HMA glaciers. Overall, there is an increase in shaded relief with increasing elevation. This is due to the increase in slope at higher elevations. However, cast shadowing does not show any clear trend with elevation; rather, it appears to be controlled by the distance, direction, and size of the immediate surrounding topography. This makes cast shadowing extremely variable along and between glaciers.

We find that glaciers with north and south valley aspects are generally more influenced by cast shadowing. Additionally, we see a general increase in shading with increasing latitude. This suggests that parameters such as latitude, aspect, slope and others may be useful in predicting the overall effect of shading for a particular glacier. This could be useful in estimating the impact of shading on a regional scale in order to incorporate shading in large-scale models.

We show that topographic shading results in a significant mean change in irradiance for certain HMA glaciers. On one of these glaciers, we calculate that summer melt was overestimated by 10% (0.8 m w.e.a^{-1}) in some areas by excluding topographic shading. This implies that topographic shading is not only an important parameter in calculating global radiation, but can also affect the overall mass balance of glaciers in HMA.

APPENDIX

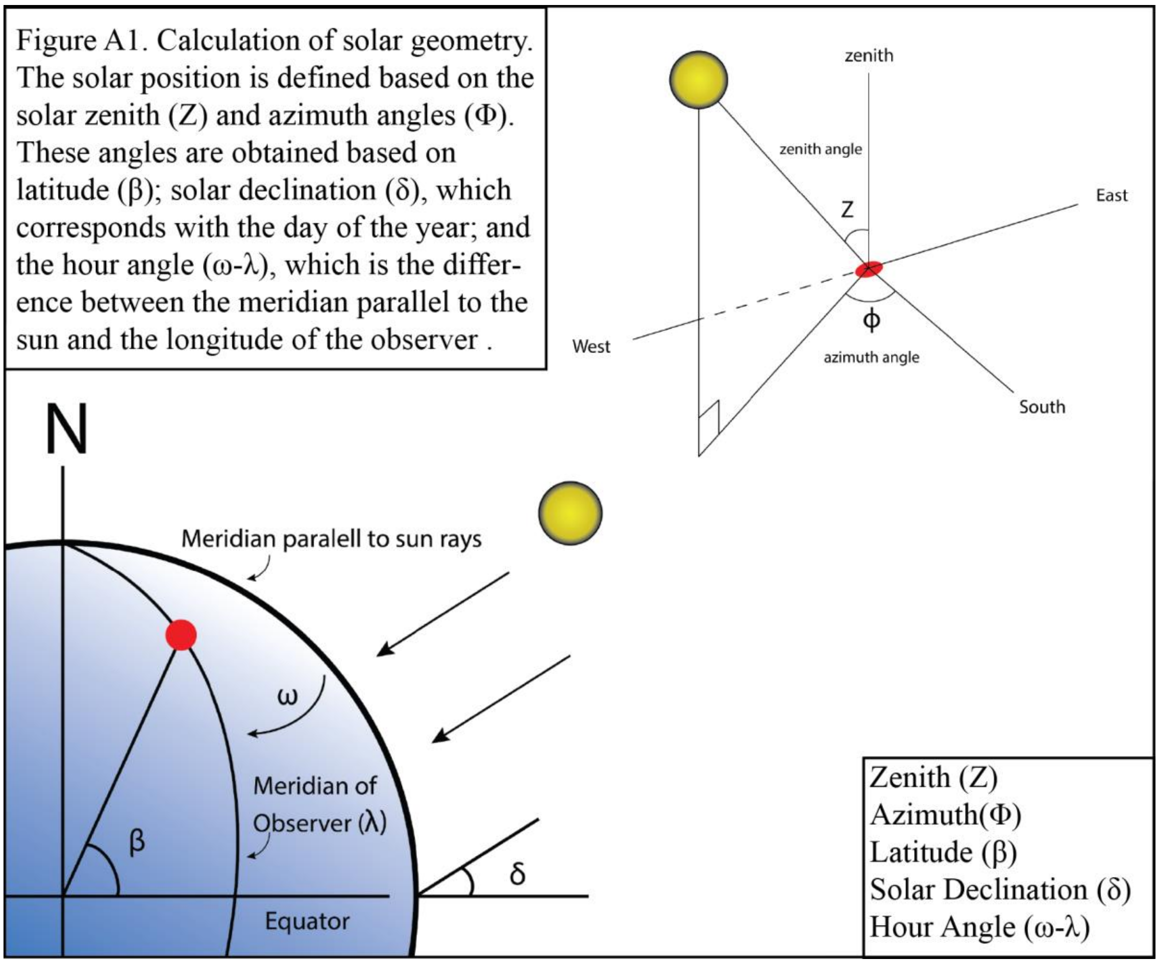

Figure A1. Calculation of solar geometry. The solar position is defined based on the solar zenith (Z) and azimuth angles (Φ). These angles are obtained based on latitude (β); solar declination (δ), which corresponds with the day of the year; and the hour angle (ω-λ), which is the difference between the meridian parallel to the sun and the longitude of the observer .

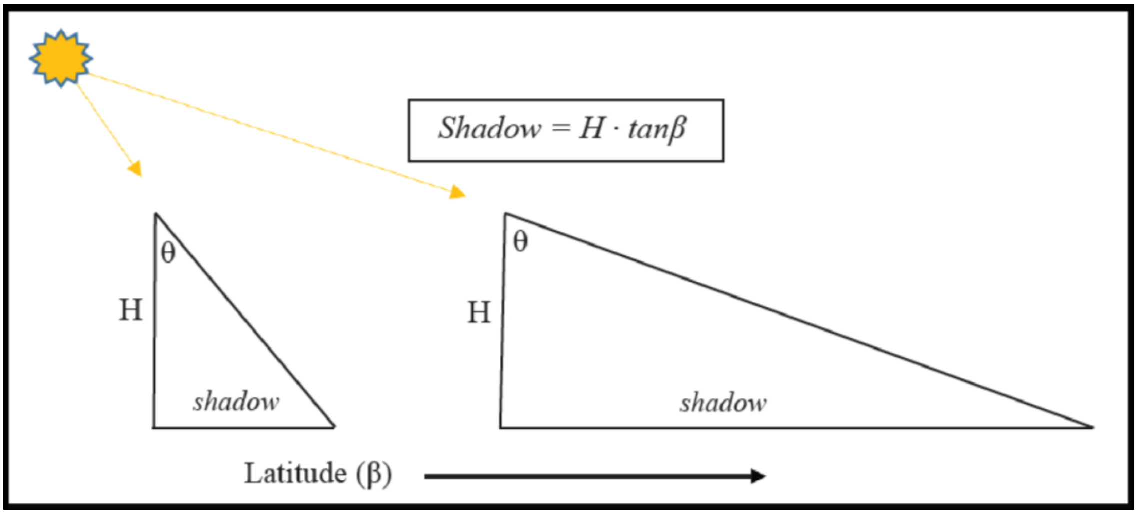

Figure A2. Illustrating the relationship between latitude and cast shadowing. As latitude increases, the zenith angle (depicted as θ) becomes larger. This causes shadow length to increase. Figure 7 shows that the relative change in irradiance received at the surface due to cast shadows can be approximated using the simple mathematical trend of one minus the tangent of the change in latitude (in degrees).

REFERENCES

Aguilar, C., Herrero, J., & Polo, M. J. (2010). Topographic effects on solar radiation distribution in mountainous watersheds and their influence on reference evapotranspiration estimates at watershed scale. *Hydrology and Earth System Sciences*, *14*(12), 2479-2494.

Arendt, A., A. Bliss, T. Bolch, J.G. Cogley, A.S. Gardner, J.-O. Hagen, … N. Zheltyhina, (2015). Randolph Glacier Inventory – A Dataset of Global Glacier Outlines: Version 5.0. *Global Land Ice Measurements from Space, Boulder Colorado, USA. Digital Media.*

Arnold, N. S., Rees, W. G., Hodson, A. J., & Kohler, J. (2006). Topographic controls on the surface energy balance of a high Arctic valley glacier. *Journal of Geophysical Research: Earth Surface*, *111*(F2), 1-15.

Bajracharya, S. R., & Shrestha, B. R. (2011). The status of glaciers in the Hindu Kush-Himalayan region. *International Centre for Integrated Mountain Development (ICIMOD).* Data accessed online on 2016-04-01 at www.icimod.org

Chen, X., Su, Z., Ma, Y., Yang, K., & Wang, B. (2013). Estimation of surface energy fluxes under complex terrain of Mt. Qomolangma over the Tibetan Plateau. *Hydrology and Earth System Sciences*, *17*(4), 1607-1618.

Corripio, J. G. (2003). Vectorial algebra algorithms for calculating terrain parameters from DEMs and solar radiation modelling in mountainous terrain. *International Journal of Geographical Information Science*, *17*(1), 1-23.

Dozier, J. (1980). A clear-sky spectral solar radiation model for snow-covered mountainous terrain. *Water Resources Research*, *16*(4), 709-718.

Dozier, J., & Frew, J. (1990). Rapid calculation of terrain parameters for radiation modeling from digital elevation data. *IEEE Transactions on Geoscience and Remote Sensing*, *28*(5), 963-969.

Duguay, C. R. (1993). Radiation modeling in mountainous terrain review and status. *Mountain Research and Development*, *13*(4), 339-357.

Evans, I. S., & Cox, N. J. (2005). Global variations of local asymmetry in glacier altitude: Separation of north–south and east–west components. *Journal of Glaciology*, *51*(174), 469-482.

Fierz, C., Riber, P., Adams, E. E., Curran, A. R., Föhn, P. M. B., Lehning, M., & Plüss, C. (2003). Evaluation of snow-surface energy balance models in alpine terrain. *Journal of Hydrology*, *282*(1), 76-94.

Flo Heggem, E. S., Etzelmüller, B., & Berthling, I. (2001). Topographic radiation balance models: Sensitivity and application in periglacial geomorphology. *Norsk Geografisk Tidsskrift-Norwegian Journal of Geography*, *55*(4), 203-211.

Frey, H., Paul, F., & Strozzi, T. (2012). Compilation of a glacier inventory for the western Himalayas from satellite data: Methods, challenges, and results. *Remote Sensing of Environment*, *124*, 832-843.

Gardner, A. S., Moholdt, G., Cogley, J. G., Wouters, B., Arendt, A. A., Wahr, J., ... Ligtenberg, S. R. (2013). A reconciled estimate of glacier contributions to sea level rise: 2003 to 2009. *Science, 340*(6134), 852-857.

Gill, K. M., Investments, F., & Merrimack, N. H. (2012). Casting shadows: Shading digital elevation models using ray tracing. *Rivier University Academic Journal*, *8*(1), 1-15.

Gueymard, C. (1987). An anisotropic solar irradiance model for tilted surfaces and its comparison with selected engineering algorithms. *Solar Energy*, *38*(5), 367-386.

Han, C., Ma, Y., Chen, X., & Su, Z. (2016). Estimates of land surface heat fluxes of the Mt. Everest region over the Tibetan plateau utilizing ASTER data. *Atmospheric Research*, *168*, 180-190.

Hock, R. (1999). A distributed temperature-index ice-and snowmelt model including potential direct solar radiation. *Journal of Glaciology*, *45*(149), 101-111.

Hock, R. (2005). Glacier melt: A review of processes and their modelling. *Progress in Physical Geography*, *29*(3), 362-391.

Hopkinson, C., Chasmer, L., Munro, S., & Demuth, M. N. (2010). The influence of DEM resolution on simulated solar radiation-induced glacier melt. *Hydrological Processes*, *24*(6), 775-788.

Immerzeel, W. W., Van Beek, L. P., & Bierkens, M. F. (2010). Climate change will affect the Asian water towers. *Science*, *328*(5984), 1382-1385.

IPCC. (2014). Climate Change 2014: Synthesis Report. Contribution of Working Groups I, II and III to the Fifth Assessment Report of the Intergovernmental Panel on Climate Change [Core Writing Team, R.K. Pachauri and L.A. Meyer (eds.)]. *IPCC, Geneva, Switzerland, 151 pp.*

Iqbal, M. (2012). *An introduction to solar radiation*. New York: Elsevier.

Jacob, T., Wahr, J., Pfeffer, W. T., & Swenson, S. (2012). Recent contributions of glaciers and ice caps to sea level rise. *Nature, 482*(7386), 514-518.

Kääb, A., Treichler, D., Nuth, C., & Berthier, E. (2015). Brief communication: Contending estimates of 2003–2008 glacier mass balance over the Pamir–Karakoram–Himalaya. *The Cryosphere*, *9*(2), 557-564.

Klok, E. J., & Oerlemans, J. (2002). Model study of the spatial distribution of the energy and mass balance of Morteratschgletscher, Switzerland. *Journal of Glaciology*, *48*(163), 505-518.

Kumar, L., Skidmore, A. K., & Knowles, E. (1997). Modelling topographic variation in solar radiation in a GIS environment. *International Journal of Geographical Information Science*, *11*(5), 475-497.

Munro, D. S., & Young, G. J. (1982). An operational net shortwave radiation model for glacier basins. *Water Resources Research*, *18*(2), 220-230.

Plummer, M. A., & Phillips, F. M. (2003). A 2-D numerical model of snow/ice energy balance and ice flow for paleoclimatic interpretation of glacial geomorphic features. *Quaternary Science Reviews*, *22*(14), 1389-1406.

Williams, L. D., Barry, R. G., & Andrews, J. T. (1972). Application of computed global radiation for areas of high relief. *Journal of Applied Meteorology*, *11*(3), 526-533.

Zhang, S., Li, X., & Chen, Y. (2015). Error assessment of grid-based direct solar radiation models. *International Journal of Geographical Information Science*, *29*(10), 1782-1806.